Green Chemistry

PAPER

View Article Online
View Journal | View Issue

Cite this: *Green Chem.*, 2021, **23**, 4044

Advanced masking agent for leather tanning from stepwise degradation and oxidation of cellulose†

Zhicheng Jiang,[a,b] Shuguang Xu,[c] Wei Ding,[d] Mi Gao,[a,b] Jiajun Fan,[e] Changwei Hu,[c] Bi Shi *[a,b] and James H. Clark *[e]

Received 12th April 2021,
Accepted 7th May 2021

DOI: 10.1039/d1gc01264a

rsc.li/greenchem

An oligosaccharide-based masking agent suitable for chrome-free metal tanning was produced from cellulose *via* a stepwise degradation and oxidation process. Firstly, an $AlCl_3$-NaCl-H_2O/γ-valerolactone (GVL) biphasic solvent system was established for cellulose conversion (87.6%), which allowed *in situ* separation of the oligosaccharides and valuable small molecules into the two phases. Then, a H_2O_2 oxidation process enabled further degradation of the oligosaccharides and introduced –CHO/–COOH groups. This process strengthened the surface charge of the oligosaccharides, enhancing their coordination ability with metal ions. The post-oxidized fraction, together with added Zr species, exhibited satisfactory tanning performance, with a shrinkage temperature of 85.2 °C for the tanned leather. Al/Zr species could spontaneously coordinate with O atoms of O=C(2) in the carboxylic group of post-oxidized oligosaccharides, which promoted the penetration of Al/Zr species into the leather matrix for efficient crosslinking reactions.

Introduction

Leather products are prepared from animal skin, which is a kind of copious and widespread natural animal biomass resource.[1] Thus, leathers can be regarded as renewable and sustainable industrial products, and they are commonly used to produce daily necessities, such as clothing, footwear and decoration.[2–4] Leather tanning is an essential step to convert raw skin into leather, and endows the leather with satisfactory mechanical strengths and high resistance to heat, chemicals and putrefaction. Specifically, leather tanning is a process which improves the dispersion and fixation of collagen fibers *via* abundant crosslinking networks between the tanning agent and $-NH_2$/–COOH groups in the collagen matrix. Tanning leather using chrome salt (Cr(III)) is the traditional and most used approach worldwide. However, as a human carcinogen is generated from the oxidation of Cr(III) to Cr(VI), chrome salts are becoming increasingly restricted due to stricter environmental regulations and health concerns.[5–7] To solve these issues, safer and eco-friendly tanning agents, such as dialdehyde polysaccharides and syntan containing chlorine groups, were prepared for leather tanning.[8,9] However, low isoelectric point of the leather tanned by organic tanning agent led to insufficient interactions with anionic dye during further treatment, resulting in poor physical property of the finished leather.[10] Apart from chrome salts, aluminum and zirconium salts also have favorable tanning performances.[11,12] It must be bared in mind that these metal tanning agents will strongly coordinate with the collagen fibers during the initial penetration process, leading to their deposition onto leather surface, non-uniform penetration and a consequently poor tanning effect.[13]

In view of this, a 'Trojan Horse strategy' was proposed in our previous work for the efficient penetration of aluminum tanning agents into collagen matrix, in which the oligosaccharides from $AlCl_3$-catalyzed degradation of cellulose were used as masking agents to coordinate with Al species.[13] However, the shrinkage temperature (T_s) of the leather tanned by this Al-oligosaccharides complex tanning agent was not high enough for commercial application, limited by the inferior tanning performance of Al species. Besides, the concentrated $AlCl_3$ aqueous solution with high acidity may easily cause repolymerization of the reaction intermediates, lowering the yield of the degraded products and increasing the molecular weight of oligosaccharides.[14,15] Given this, the objective of this work is to establish a biphasic $AlCl_3$-NaCl-H_2O/

[a]College of Biomass Science and Engineering, Sichuan University, Chengdu, 610065, P. R. China. E-mail: shibi@scu.edu.cn; Fax: +86-28-85400356; Tel: +86-28-85400356
[b]National Engineering Research Center of Clean Technology in Leather Industry, Sichuan University, Chengdu, 610065, P. R. China
[c]Key Laboratory of Green Chemistry and Technology, Ministry of Education, Sichuan University, Chengdu, 610065, P. R. China
[d]China Leather and Footwear Research Institute Co. Ltd., Beijing, 100015, P. R. China
[e]Green Chemistry Centre of Excellence, Department of Chemistry, University of York, York, YO10 5DD, UK. E-mail: james.clark@york.ac.uk

†Electronic supplementary information (ESI) available. See DOI: 10.1039/d1gc01264a

γ-valerolactone (GVL) co-solvent system for the conversion of cellulose and *in situ* separation of the generated products to prevent the side-chain reactions, obtaining high-quality 'oligosaccharide-based masking agent' for leather tanning and valuable platform chemicals simultaneously. To enhance the masking effect of the oligosaccharides for metal ions penetration, the prepared oligosaccharides were further oxidized so as to introduce more active coordination groups. Additionally, Zr species with stronger crosslinking ability was employed together with Al species to improve the performance of tanned leather. This renewable and eco-friendly Al–Zr-oligosaccharides complex with satisfactory tanning performance can be regarded as an advanced and alternative tanning agent, thereby eliminating Cr discharge and promoting the sustainable development of the leather industry.

Results and discussion

Biphasic solvent system

Several biphasic solvent systems were established using $AlCl_3$-NaCl-H_2O as catalytic reaction phase, where ethyl acetate (EtOAc), *n*-butyl alcohol (*n*-BuOH), tetrahydrofuran (THF), 2-methytetrahydrofuran (MeTHF) and γ-valerolactone (GVL) were employed as *in situ* extraction phase, respectively. The aqueous solution with concentrated salts lowers the solubility of the organic solvent in water, and a biphasic co-solvent system was generated, in which the reaction products can spontaneously dissolve in the H_2O and organic phases according to the partition coefficients.[16–18] Then, the conversion of microcrystalline cellulose was investigated in the above biphasic systems at 200 °C using an Anton Paar microwave reactor. As presented in Fig. 1, all these catalytic co-solvent systems showed good performance in cellulose conversion, with 75% to 90% conversion rates. After the reaction, the oligosaccharides were the predominant products in the hydrolysates, followed by levulinic acid (LeA), formic acid (FA), acetic acid (AA), lactic acid (LaA) and HMF. For the biphasic solvent systems, *in situ* extraction of the generated small molecule products can prevent their further decomposition or repolymerization. For example, THF can efficiently separate HMF *via* hydrogen bonding interaction with HMF, avoiding its hydrolysis into levulinic acid and formic acid, as a result, the yield of HMF in the $AlCl_3$-NaCl-H_2O/GVL was higher.[16] For $AlCl_3$-NaCl-H_2O/MeTHF system, the generated carboxylic acids and furans can be transferred into the MeTHF phase immediately due to the extraordinary phase splitting, leading to higher yields of small molecular products. In contrast, a more balanced distribution of the products was obtained using the $AlCl_3$-NaCl-H_2O/GVL biphasic solvent system, in which half of the converted cellulose was decomposed to small molecule products distributed in the two phases and the remaining half was maintained as the oligosaccharides in H_2O phase. However, only 49.7% of the small molecule products were distributed in GVL phase after the solvothermal reaction. To further purify the tanning agent and obtain small molecule products, additional extractions proceeded for efficient production separation, and the aforementioned proportion of small molecule products in the GVL phase could be substantially increased to 85.5%. Noticeably, LeA, FA and HMF occupied 89.7% of the identified small molecule products in GVL; these chemicals are the starting materials to be further synthesized into GVL *via* hydrogenation,[19,20] potentially achieving GVL regeneration as the reaction solvent.

The aqueous fraction rich in Al^{3+} ions and oligosaccharides could be considered as a potential metal complex tanning agent.[21,22] The tanning performance of the H_2O fractions produced in the different biphasic co-solvent systems were tested using pickled cattleskin as the raw material in a drum. T_s and color difference (ΔE, lower ΔE value generally means higher whiteness of the tanned leather) were examined, where the former is an important parameter to characterize the tanning performance and the latter is closely related to the flexibility of leather for commercial use.[2,10,21] Approximately 64 °C for T_s was obtained for the leathers tanned by H_2O fractions from *n*-BuOH-adopted and GVL-adopted reaction systems, slightly higher than that of untanned cattle skin (56.8 °C), indicating better tanning effects of these two H_2O fractions. Furthermore, the ΔE of the tanned leather from GVL-adopted experiment was 23.4%, which was obviously lower than that from *n*-BuOH-adopted experiment, presenting higher whiteness for further application. Under comprehensive evaluation, $AlCl_3$-NaCl-H_2O/GVL biphasic system was selected for the catalytic conversion

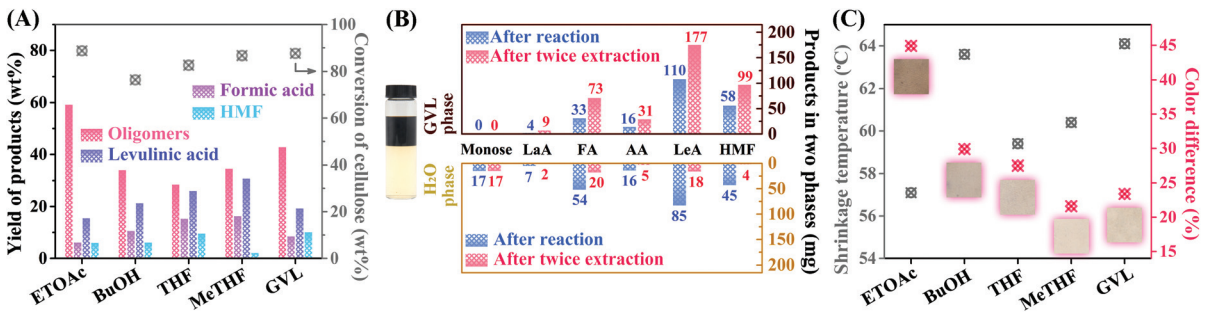

Fig. 1 (A) Effect of different biphasic solvent systems on the conversion of cellulose and yield of products catalyzed by $AlCl_3$ at 200 °C for 20 min; (B) distribution of the small molecule products in the two phases after reaction and with twice additional extraction. (C) T_s and color difference of the leather tanned by the H_2O fraction after reaction.

of cellulose to produce a tanning agent in the H_2O phase and valuable chemicals in the GVL phase.

H_2O_2 oxidation of the oligosaccharides

Limited by the unsatisfactory tanning performance of Al species, the relatively low T_s of the Al-tanned leather cannot meet the commercial requirements. Owing to the excellent crosslinking ability, Zr species was directly introduced into the obtained hydrolysate to improve the tanning effect. Meanwhile, stronger coordination ability of Zr species brought about the severe overload of metal ions on leather surface, hindering its penetration and attenuating the tanning effect. However, the oligosaccharides from cellulose degradation, with dominant –OH groups and consequently low coordination ability, were ineffective for the masking effect on the penetration of Zr species. Thus, the obtained oligosaccharides in H_2O phase from $AlCl_3$-NaCl-H_2O/GVL reaction systems were further oxidized by H_2O_2 using Cu–Fe catalyst to introduce diverse oxygen-containing groups,[22] which can easily coordinate with metal ions and favor their effective penetration into the collagen fiber matrix. As shown in Fig. 2, more –CHO and –COOH groups were generated in the oligosaccharides with the increasing concentration of H_2O_2. For example, only 1 vol% of H_2O_2 could produce 21.1 mmol L^{-1} of –COOH group, which is nearly 8 times more than that in the original hydrolysates before oxidation.

Besides, oxidation of the oligosaccharides also brought about molecular weight with a relatively intensive distribution of the oxidized oligosaccharides. Owing to more –CHO/–COOH randomcleavage of the glycosidic bonds, leading to lower groups and smaller molecular weight, the oxidized oligosaccharides exhibited much better masking performance to promote the penetration of Al and Zr species, and a substantially higher T_s was obtained for the tanned leather. Although excessively strong masking effect of the over-oxidized oligosaccharides obtained from the relatively concentrated H_2O_2 solution helped the penetration of metal ions into the collagen matrix, it is unfavorable for the release of metal ions from the 'metal-oligosaccharides complex' for further crosslinking reactions with the –COOH on collagen fibers, slightly decreasing T_s of the tanned leather. Besides, decoloring the cellulose-derived reaction fluid was another significant function of the H_2O_2 oxidation process, whitening the tanned leather with a low color difference and enlarging its potential application.

To evaluate the masking effect of the oligosaccharides ligands on the tanning performance, different cellulose dosages were used for the preparation of metal-oligosaccharides tanning agents (Fig. S1 and S2†). Compared to a much lower T_s of the leather tanned by Al/Zr tanning agent, relatively higher T_s of the leather tanned by Al/Zr-oligosaccharide complex tanning agent confirmed the masking effect of the oligosaccharides. However, with a higher concentration of cellulose, the concentrated oligosaccharides produced led to their repolymerization into macromolecules, which hindered the penetration of metal-oligosaccharides complex and weakened the tanning effect with low T_s of the tanned leather.

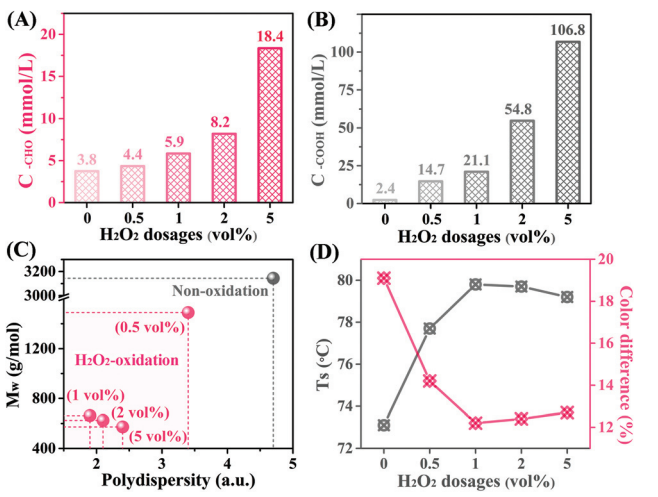

Fig. 2 Concentration of (A) aldehyde groups and (B) carboxyl groups in the different oxidized H_2O fraction from $AlCl_3$-NaCl-H_2O/GVL reaction system. (C) Average molecular weight and polydispersity of the oxidized oligomers with different oxidation degree. (D) Effect of H_2O_2 dosages on shrinkage temperature and color difference of the leather tanned by the Al–Zr-oxidized oligomers tanning agents.

Masking mechanism of the oligosaccharides

To gain a deep insight into the masking behavior of the coordination between Al/Zr species and the oligosaccharides, computational simulations were conducted. According to the literature, H_2O_2 oxidation of the cellulose-derived oligosaccharides undergo two pathways: one is the oxidation of C6–OH into –COOH group (C6-oxidation), and the other one is the oxidation of C2–C3 bonds to generate two –COOH groups with ring open reaction (C2,3-oxidation).[23] Therefore, the oxidized cellotriose composed of an unoxidized glucose, a C6-oxidized glucose and a C2,3-oxidized glucose, was selected as a model compound during the theoretical computation experiments (Fig. 3). Before investigating the coordination behavior, the surface charge density of the oxidized cellotriose was analyzed to reveal the probable coordination sites. More electronic density was accumulated on the O atom in the oxidized cellotriose, wherein the electronic density around the C═O bonds in –COOH groups at C2, C3 and C6 was much stronger than that around –OH groups. This confirmed the fact that H_2O_2 oxidation could strengthen the surface charge density of the oligosaccharides, and Al/Zr species would coordinate with the –COOH groups in preference.

Then, $[Al(OH)_2(aq)]^+$ and $[Zr(OH)_2(aq)]^{2+}$ were chosen as the active Al/Zr species in the tanning agent according to the literatures.[13,14,24] Due to the strong surface charge density of the O atoms in –COOH groups, several coordination modes of Al/Zr species on the C═O were simulated. At room temperature, $[Al(OH)_2(H_2O)_2]^+$ and $[Zr(OH)_2(H_2O)_2]^{2+}$ species could coordinate with O═C(2), O═C(3) or O═C(6) of the –COOH groups in the oxidized cellotriose separately with negative ΔG values, and Al/Zr species could also coordinate with O═C(2)

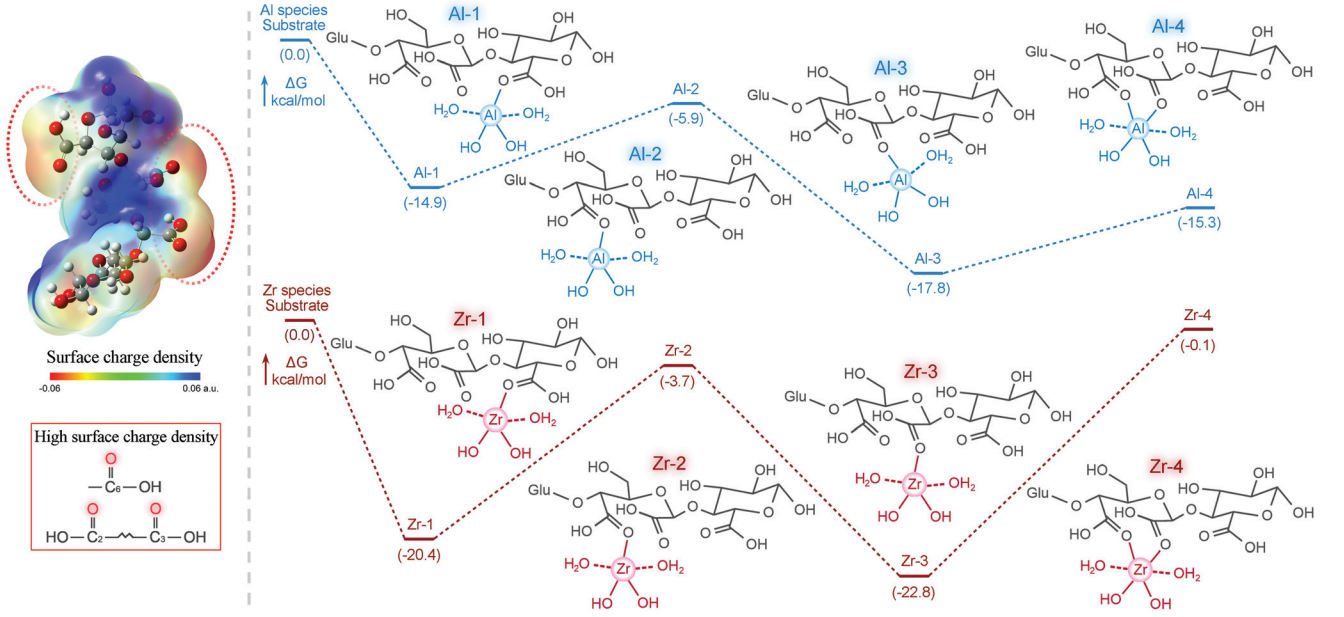

Fig. 3 Surface charge density analysis of the oxidized oligosaccharides, and energy profiles for the interactions of Al/Zr species and the oxidized oligosaccharides.

and O=C(3) simultaneously. In comparison, both Al and Zr species preferred to coordinate with O=C(2), with the lowest ΔG of −17.8 and −22.8 kcal mol^{-1}, respectively. Therefore, the spontaneous coordination of Al/Zr species and the oxidized oligosaccharides mitigated the overload of Al/Zr species on the leather surface and promote the penetration of Al/Zr species into the leather matrix. The penetrated Al/Zr species could further be released from the Al/Zr-oligosaccharides complex and coordinated with –COOH/–NH_2 groups on the collagen fibers by changing the pH value of the tanning agent, dispersing and stablizing the collagen fibers.

These representations reveal that the T_s of the tanned leather depends on the catalytic temperature used in the synthesis step. At low temperature (100 °C), regardless of the $AlCl_3$ and H_2O_2 concentrations, the tanned leather T_s is lower than 80 °C. However, an increase in the temperature leads to an enhancement in the T_s up to around 90 °C, thus making this product appropriate to meet the restrictive requirements for commercial application. Such enhancement in the T_s of the tanned leather goes in line with the increases observed for the hemicellulose conversion when the hydrothermal synthesis temperature increases. Thus, this development helps to prove evidence for the core effect of the xylo-oligosaccharides concentration on the tanning performance of our 'advanced Trojan horse' tanning agent.

Masking effect of the oligosaccharides

In order to visually observe the penetration efficiency of Al and Zr species assisted by the oligosaccharides, a series of the Al/Zr-oligosaccharides complex tanning agents with different Al/Zr proportions were subjected to tanning tests (Fig. 4). To better describe the dosages of Al and Zr species during the tanning procedure, their concentrations were calculated as Al_2O_3 and ZrO_2 based on the use of $AlCl_3$ and $Zr(SO_4)_2$. The T_s of the leathers tanned by 0.5 wt% Al_2O_3–2 wt% ZrO_2 tanning agent was only 70.4 °C, and increasing Al_2O_3 concentration to 1.5 wt% resulted in a raised T_s to 81.1 °C. From stereo microscope images taken, smoother grain and clearer pores could be observed for the leather tanned with 1.5 wt% of Al_2O_3. Meanwhile, a higher dispersion of the collagen fibers and a more uniform distribution of metals in the grain, middle and flesh sides, indicated a more efficient and uniform penetration of metals in leather. However, further increasing Al_2O_3 concentration caused a relatively rough grain surface, a substantial agglomeration of the collagen fibers and the intensive accumulation of metals on the two outer layers of the tanned leather, which revealed the ineffective penetration of metal ions. It could be ascribed to that the oligosaccharides with higher molecular weight were formed *via* repolymerization in the more concentrated $AlCl_3$ reaction system (Fig. S3†), and the metal-oligosaccharides complexes with larger size hindered their penetration into the leather matrix. Besides, 67.5 °C of T_s was obtained for the tanned leather using 1.5 wt% Al_2O_3–0 wt% ZrO_2 tanning agent, demonstrating the significant tanning effect of both Al and Zr species. In particular, an obviously competitive absorption of Al and Zr species onto collagen fibers could be observed with different concentrations of Al_2O_3 and ZrO_2. That is to say, an upward absorption value of one metal always accompanied a downward absorption value of another, and *vice versa* (Fig. 4B). This might show that the constant active sites in the oxidized oligosaccharides are competitively coordinated with these two metal species for their further penetration. Coincidentally, the absorption of carbon is positively correlated with the absorption of Zr, rather than

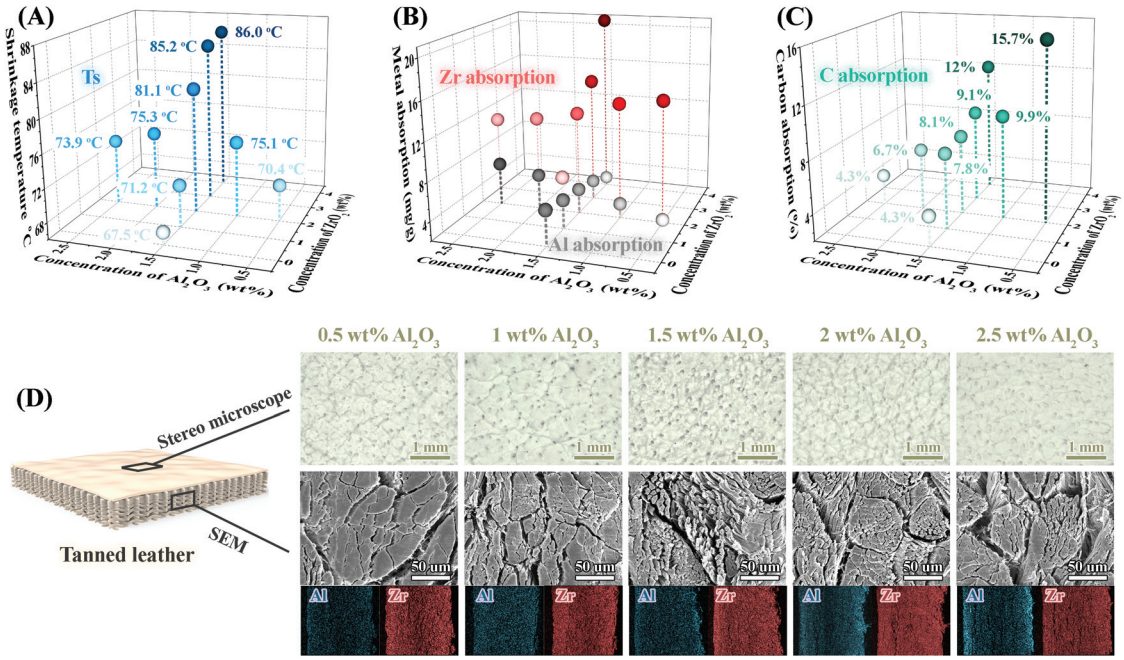

Fig. 4 Effects of Al_2O_3–ZrO_2 concentration on (A) T_s of the tanned leather, (B) metal absorption and (C) carbon absorption during tanning process; (D) stereomicroscope images of the grain surface, SEM and Al–Zr mapping images of the cross-section.

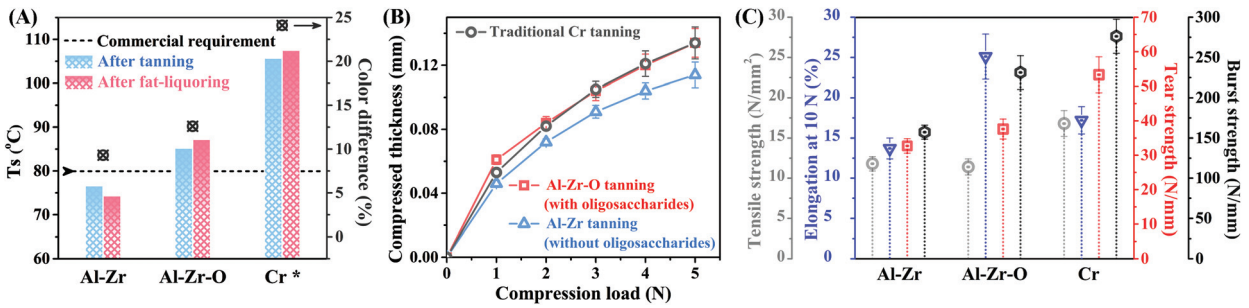

Fig. 5 (A) T_s of the leather after tanning and further after fat-liquoring, and color difference of the leather after tanning; (B) compression performance curve, (C) physical and mechanical properties of the leather after fat-liquoring. *T_s of Cr-tanned leather was detected in glycerol.

the absorption of Al, deducing stronger coordination of Zr-oligosaccharides than Al-oligosaccharides.

Physical properties of the tanned leather

To evaluate the application potential of the resultant leather, the performance of the as-prepared Al–Zr-oligosaccharides (Al–Zr–O) tanned leather, oligosaccharides-free Al–Zr tanned leather and traditional Cr-tanned leather were characterized and compared (Fig. 5). Both traditional Cr-tanned and Al–Zr–O tanned leathers met the general T_s requirement (>80 °C) for commercial use,[25] whereas T_s of Al–Zr tanned leather was only 76.6 °C. Furthermore, the subsequent retanning and fat-liquoring process slightly increased the T_s of the two former leathers, while the T_s of the latter leather reduced after these procedures. This revealed that the oxidized oligosaccharides can stabilize the metals in collagen matrix by complicated oligosaccharides-Al–Zr-collagen fibers networks, hence preventing de-tanning during the industrial follow-up process. Cr-tanned leather is commonly regarded to have outstanding organoleptic and mechanical properties. Although the overall mechanical properties (tensile strength, tear strength and burst strength) of Al–Zr–O tanned leather were incomparable to those of Cr-tanned leather, this Cr-free tanned leather showed acceptable fullness and elongation, mainly attributing to the favorable filling effect of the oligosaccharides in the collagen matrix. Thus, the leather product tanned by the Al–Zr-oligosaccharides complex can meet the general requirements for commercial use and can be applied in the sustainable leather industry.

Conclusions

In this paper, the conversion of microcrystalline cellulose was conducted in a biphasic $AlCl_3$-NaCl-H_2O/GVL co-solvent

system at 200 °C, and 87.6% of cellulose was converted into the oligosaccharides and small molecule products (half-and-half). 85.5% of the small molecule products were dissolved in the GVL phase, while most of the oligosaccharides were retained in the H_2O phase. Further H_2O_2 oxidation of the oligosaccharides in the H_2O phase broke the glycosidic bonds, and the M_w of the oligosaccharides substantially decreased from 3144 g mol^{-1} to about 600 g mol^{-1}. Besides, –CHO and –COOH groups were introduced *via* H_2O_2 oxidation, strengthening the surface charge density of the oligosaccharide and improving their coordination ability with metal ions as a consequence. Al and Zr species could competitively coordinate with the limited –COOH group at C2 in the oxidized oligosaccharides. Then, the Al/Zr-oligosaccharides complex could easily penetrate into leather matrix, and the collagen fibers would be well dispersed and stabilized *via* crosslinking reactions between immersed Al/Zr species and the collagen fibers. With satisfactory T_s and mechanical strength, the resultant leather exhibited great potential for commercial use.

Experimental

Materials

Microcrystalline cellulose, $AlCl_3{\cdot}6H_2O$, 30% H_2O_2, $Zr(SO_4)_2{\cdot}4H_2O$, NaCl were purchased from Sigma-Aldrich and Aladdin and used as received. Pickled cattle pelt was purchased from Haining Ruixing Leather Co., Ltd, China.

Microwave-assisted cellulose conversion

Microcrystalline cellulose, $AlCl_3{\cdot}6H_2O$ and NaCl were placed equally in four 100 mL microwave Teflon tubes. 50 mL reaction solvent, including 35 mL distilled water and 15 mL organic solvent was mixed in each tubes. The reaction tubes were sealed and heated using an Anton Paar microwave with continuous stirring. Temperature was monitored inside the reaction tube using a Ruby probe. Each reaction was heated from room temperature to 200 °C within 10 min, and held for differing periods. When the reaction was finished, the reaction system was cooled down below 50 °C using compressed air. The reaction slurry was filtered to separate the solid residue from the liquid fraction. The collected solid residue was dried in an oven at 105 °C overnight for conversion calculation. The biphasic liquid fraction was transferred into separatory funnel for phase splitting to obtain the aqueous fraction and organic fraction.

Tanning process

Before tanning process, the oligosaccharides was subjected to a H_2O_2 oxidation treatment. Specifically, the aqueous fraction and a certain amount of H_2O_2 with traditional Cu–Fe catalyst were heated with reflux condensation at 90 °C for 2 h.[22] Pickled cattle pelt was tailored along the back bone into matched pieces. Then they were tanned with the post-oxidized aqueous fraction at 1 : 2 weight ratio based on the weight of pickled pelt, and additional $Zr(SO_4)_2{\cdot}4H_2O$ (equally to 2 wt% of ZrO_2) was added. After running for 4 h in a drum, the pH of tanning liquor was adjusted to around 4.0 with $NaHCO_3$ solution with 3 h. The drum kept running for 4 h at 40 °C and then stood for 12 h for the sufficient crosslinking between tanning agent and collagen fiber. The resultant tanned leather was finally washed by running water at room temperature to remove the residual tanning agent, and then dried in the air.

Characterization of liquid products in the tanning agent

The small molecule products were quantitatively measured by high-performance liquid chromatography (HPLC, Agilent) with RI detectors. 0.5 mM H_2SO_4 solution was used as mobile phase at a flow rate of 0.6 mL min^{-1}. The molecular weight distribution of the oligosaccharides in the H_2O phase was analyzed using gel permeation chromatography (GPC, Agilent) with a PL aquagel-OH column and a RI detector, and ultrapure water was used as the mobile phase at a flow rate of 1.0 mL min^{-1}. –CHO and –COOH contents in the oligosaccharides were quantitatively analyzed using hydroxyl amine method and NaOH chemical titrations.

Chemical and physical testing of the tanned leather and the post tanning agent

The shrinkage temperature (T_s) of the tanned leather was measured and recorded using a digital leather shrinkage temperature instrument (MSW-YD4, Shaanxi University of Science and Technology, China). The solvent was water and the heating rate was kept at 2 °C min^{-1}. After freeze drying to remove the moisture of leather, the cross section of the tanned leather was observed using scanning electron microscope (SEM, JSM-7500F, JEOL) equipped with energy-dispersive spectrometry (EDS) analysis. The grain surface of the tanned leather was observed using stereo microscope (SZX12, Olympus). Color measurement parameters (L, a, b) of the tanned leather were recorded using a color measurement instrument (Color reader CR-13, Konica Minolt). The total color difference (ΔE) was calculated based on the standard white card. Before mechanical strength analysis, the dried curst leather samples were firstly air conditioned for 48 h at 20 °C and 65% RH. Then, the tensile and tear strengths of curst leather were determined according to the standard methods using a tensile tester (AI-7000SN, Gotech).

Computational details

Full geometry optimizations in aqueous solution were performed to locate all the stationary points, using the PBE0 method,[26] with the 6-31G(d) basis set for Al, C, H and O atoms,[27] lanlzdz for Zr atom, namely PBE0/6-31G(d), lanl2dz. The self-consistent reaction field method based on the universal solvation model SMD was adopted to evaluate the effect of the solvent.[28] Unless otherwise specified, the Gibbs free energy of formation (ΔG) is relative to the initial reactants including ZPE correction obtained at the PBE0/6-31G(d), lanl2dz level. All geometry calculations were run with the Gaussian 09 program. Electrostatic potential analysis (ESP) was performed on the molecular van der Waals (vdW) surface.[29]

Conflicts of interest

There are no conflicts to declare.

Acknowledgements

This work is financially supported by the National Natural Science Foundation of China (22078211), Sichuan Science and Technology Program (2020YJ0023). We also appreciate Hui Wang from the Analytical & Testing Center of Sichuan University for her help with SEM characterization. We also thank Dr Xiu He at College of Biomass Science and Engineering, Sichuan University, for experimental assistance.

References

1 L. He, C. Mu, J. Shi, Q. Zhang, B. Shi and W. Lin, *Int. J. Biol. Macromol.*, 2011, **48**, 354–359.
2 L. Rosu, C. D. Varganici, A. M. Crudu, D. Rosu and A. Bele, *J. Cleaner Prod.*, 2018, **177**, 708–720.
3 C. Liu, N. P. Latona, R. Ashby and K. Ding, *J. Am. Leather Chem. Assoc.*, 2006, **101**, 368–375.
4 X. Wang, Y. Tang, Y. Wang, L. Ke, X. Ye, X. Huang and B. Shi, *Chem. Eng. Sci.*, 2019, **196**, 64–71.
5 R. Chaudhary and A. Pati, *J. Am. Leather Chem. Assoc.*, 2016, **111**, 10–16.
6 B. Wu, S. Yu, G. Zhang, S. Zhang, P. Shen and P. G. Tratnyek, *J. Hazard. Mater.*, 2020, **400**, 123306.
7 B. Li, P. Liao, L. Xie, Q. Li, C. Pan, Z. Ning and C. Liu, *Water Res.*, 2020, **181**, 115923.
8 L. Yu, X. Qiang, L. Cui, B. Chen, X. Wang and X. Wu, *J. Cleaner Prod.*, 2020, **270**, 122351.
9 N. Ariram and B. Madhan, *J. Cleaner Prod.*, 2020, **250**, 119441.
10 W. Ding, Y. Yi, Y. Wang, J. Zhou and B. Shi, *Carbohydr. Polym.*, 2019, **224**, 115169.
11 K. H. Sizeland, H. C. Wells, R. L. Edmonds, N. Kirby and R. G. Haverkamp, *J. Am. Leather Chem. Assoc.*, 2016, 391–397.
12 S. Cao, Y. H. Zeng, B. Z. Cheng, W. H. Zhang and B. Liu, *J. Am. Leather Chem. Assoc.*, 2016, 242–249.
13 Z. Jiang, W. Ding, S. Xu, J. Remón, B. Shi, C. Hu and J. H. Clark, *Green Chem.*, 2020, **22**, 316–321.
14 J. Tang, X. Guo, L. Zhu and C. Hu, *ACS Catal.*, 2015, **5**, 5097–5103.
15 X. Fu, J. Dai, X. Guo, J. Tang, L. Zhu and C. Hu, *Green Chem.*, 2017, **19**, 3334–3343.
16 Z. Jiang, P. Zhao, J. Li, X. Liu and C. Hu, *ChemSusChem*, 2018, **11**, 397–405.
17 Z. Jiang, J. Remón, T. Li, V. L. Budarin, J. Fan, C. Hu and J. H. Clark, *Cellulose*, 2019, **26**, 8383–8400.
18 J. Fan, M. De bruyn, V. L. Budarin, M. J. Gronnow, P. S. Shuttleworth, S. Breeden, D. J. Macquarrie and J. H. Clark, *J. Am. Chem. Soc.*, 2013, **135**, 11728–11731.
19 Y. Luo, J. Yi, D. Tong and C. Hu, *Green Chem.*, 2016, **18**, 848–857.
20 S. Dutta, I. K. M. Yu, D. C. W. Tsang, Y. H. Ng, Y. S. Ok, J. Sherwood and J. H. Clark, *Chem. Eng. J.*, 2019, **372**, 992–1006.
21 W. Ding, Y. Wang, J. Zhou and B. Shi, *Carbohydr. Polym.*, 2018, **201**, 549–556.
22 Y. Yu, Y. Wang, W. Ding, J. Zhou and B. Shi, *Carbohydr. Polym.*, 2017, **174**, 823–829.
23 Q. Li, A. Wang, K. Long, Z. He and R. Cha, *ACS Sustainable Chem. Eng.*, 2018, **7**, 1129–1136.
24 M. He, H. Fu, B. Su, H. Yang, J. Tang and C. Hu, *J. Phys. Chem. B*, 2014, **118**, 13890–13902.
25 W. Ding, X. Pang, Z. Ding, D. C. W. Tsang, Z. Jiang and B. Shi, *J. Hazard. Mater.*, 2020, **396**, 122771.
26 C. Adamo and V. Barone, *J. Chem. Phys.*, 1999, **110**, 6158–6170.
27 R. Krishnan, J. S. Binkley, R. Seeger and J. A. Pople, *J. Chem. Phys.*, 1980, **72**, 650–654.
28 A. V. Marenich, C. J. Cramer and D. G. Truhlar, *J. Phys. Chem. B*, 2009, **113**, 4538–4543.
29 J. S. Murray and P. Politzer, *Wiley Interdiscip. Rev.: Comput. Mol. Sci.*, 2011, **1**, 153–163.

